Enhancing signal detection and completely eliminating scattering using quasi-phase-cycling in 2D IR experiments

Robbert Bloem,[1] **Sean Garrett-Roe,**[1] **Halina Strzalka, Peter Hamm,**[1,*] **Paul Donaldson**[1,2]

[1]*Physical Chemistry Institute, University of Zürich, Winterthurerstrasse 190, 8057 Zurich, Switzerland*

[2]*p.m.donaldson@pci.uzh.ch*

[*]*p.hamm@pci.uzh.ch*

Abstract: We demonstrate how quasi-phase-cycling achieved by sub-cycle delay modulation can be used to replace optical chopping in a box-CARS 2D IR experiment in order to enhance the signal size, and, at the same time, completely eliminate any scattering contamination. Two optical devices are described that can be used for this purpose, a wobbling Brewster window and a photoelastic modulator. They are simple to construct, easy to incorporate into any existing 2D IR setup, and have attractive features such as a high optical throughput and a fast modulation frequency needed to phase cycle on a shot-to-shot basis.

OCIS codes: (120.6200) Spectrometers and spectroscopic instrumentation; (320.7150) Ultrafast spectroscopy; (300.6300) Spectroscopy, fourier transforms.

References and links

1. S. Mukamel and R. M. Hochstrasser, "2D spectroscopy," Chem. Phys. **266**, 135–136 and all articles in that issue (2001).
2. R. M. Hochstrasser, "Multidimensional ultrafast spectroscopy," Proc. Natl. Acad. Sci. USA **104**, 14189 and all articles in that issue (2007).
3. S. Mukamel, Y. Tanimura, and P. Hamm, "Coherent multidimensional optical spectroscopy," Acc. Chem. Research **42**, 1207–1209 and all articles in that issue (2009).
4. S. Mukamel, "Multidimensional femtosecond correlation spectroscopies of electronic and vibrational excitations," Annu. Rev. Phys. Chem. **51**, 691–729 (2000).
5. P. Hamm and R. M. Hochstrasser, "Structure and dynamics of proteins and peptides: Femtosecond two-dimensional infrared spectroscopy," in *Ultrafast Infrared and Raman Spectroscopy*, M. D. Fayer, ed. (Marcel Dekker, New York, 2001), pp. 273–347.
6. M. T. Zanni and R. M. Hochstrasser, "Two-dimensional infrared spectroscopy: a promising new method for the time resolution of structures," Curr. Opin. Struct. Biol. **11**, 516–522 (2001).
7. N. H. Ge and R. M. Hochstrasser, "Femtosecond two-dimensional infrared spectroscopy: IR-COSY and THIRSTY," Phys. Chem. Comm. **5**, 17–26 (2002).
8. S. Woutersen and P. Hamm, "Nonlinear 2D vibrational spectroscopy of peptides," J. Phys.: Condens. Matter **14**, R1035–R1062 (2002).
9. D. M. Jonas, "Two-dimensional femtosecond spectroscopy," Ann. Rev. Phys. Chem. **54**, 425–463 (2003).
10. M. Cho, "Coherent two-dimensional optical spectroscopy," Bull. Korean Chem. Soc. **27**, 1940–1960 (2006).
11. J. Zheng, K. Kwak, and M. D. Fayer, "Ultrafast 2D IR vibrational echo spectroscopy," Acc. Chem. Research **40**, 75–83 (2007).
12. J. Bredenbeck, J. Helbing, C. Kolano, and P. Hamm, "Ultrafast 2D-IR spectroscopy of transient species," ChemPhysChem **8**, 1747–1756 (2007).

#136705 - $15.00 USD Received 20 Oct 2010; revised 11 Nov 2010; accepted 16 Nov 2010; published 8 Dec 2010

13. I. J. Finkelstein, J. Zheng, H. Ishikawa, S. Kim, K. Kwak, and M. D. Fayer, "Probing dynamics of complex molecular systems with ultrafast 2D IR vibrational echo spectroscopy," Phys. Chem. Chem. Phys. **9**, 1533–1549 (2007).
14. P. Hamm, J. Helbing, and J. Bredenbeck, "Two-dimensional infrared spectroscopy of photoswitchable peptides," Annu. Rev. Phys. Chem. **59**, 291–317 (2008).
15. Z. Ganim, H. S. Chung, A. W. Smith, L. P. DeFlores, K. C. Jones, and A. Tokmakoff, "Amide I two-dimensional infrared spectroscopy of proteins," Acc. Chem. Res. **41**, 432–441 (2008).
16. Y. S. Kim and R. M. Hochstrasser, "Applications of 2D IR spectroscopy to peptides, proteins, and hydrogen-bond dynamics," J. Phys. Chem. B **113**, 8231–8251 (2009).
17. M. Cho, *Two-Dimensional Optical Spectroscopy* (CRC Press, Boca Raton, 2009).
18. S. H. Shim and M. T. Zanni, "How to turn your pump-probe instrument into a multidimensional spectrometer: 2D IR and Vis spectroscopies via pulse shaping," Phys. Chem. Chem. Phys. **11**, 748–761 (2009).
19. P. Hamm and M. T. Zanni, *Concepts and Methods of 2D Infrared Spectrsocopy* (Cambridge University Press, Cambridge, 2011).
20. E. R. Andresen, R. Gremaud, A. Borgschulte, A. J. Ramirez-Cuesta, A. Züttel, and P. Hamm, "Vibrational dynamics of $LiBH_4$ by infrared pump-probe and 2D spectroscopy," J. Phys. Chem. A **113**, 12838–12846 (2009).
21. S. H. Shim, D. B. Strasfeld, Y. L. Ling, and M. T. Zanni, "Automated 2D IR spectroscopy using a mid-IR pulse shaper and application of this technology to the human islet amyloid polypeptide," Proc. Natl. Acad. Sci. USA **104**, 14197–14202 (2007).
22. D. Keusters, H. Tan, and W. Warren, "Role of pulse phase and direction in two-dimensional optical spectroscopy," J. Phys. Chem. A **103**, 10369–10380 (1999).
23. W. DeBoeij, M. Pshenichnikov, and D. Wiersma, "Phase-locked heterodyne-detected stimulated photon echo. A unique tool to study solute-solvent interactions," Chem. Phys. Lett. **238**, 1–8 (1995).
24. A. Albrecht, J. Hybl, S. Faeder, and D. M. Jonas, "Experimental distinction between phase shifts and time delays: Implications for femtosecond spectroscopy and coherent control of chemical reactions," J. Chem. Phys. **111**, 10934–10956 (1999).
25. P. Tian, D. Keusters, Y. Suzaki, and W. Warren, "Femtosecond phase-coherent two-dimensional spectroscopy," Science **300**, 1553–1555 (2003).
26. P. Tekavec, G. Lott, and A. Marcus, "Fluorescence-detected two-dimensional electronic coherence spectroscopy by acousto-optic phase modulation," J. Chem. Phys. **127**, 214307 (2007).
27. E. M. Grumstrup, S.-H. Shim, M. A. Montgomery, N. H. Damrauer, and M. T. Zanni, "Facile collection of two-dimensional electronic spectra using femtosecond pulse-shaping technology," Optics Express **15**, 16681 (2007).
28. J. A. Myers, K. L. M. Lewis, P. F. Tekavec, and J. P. Ogilvie, "Two-color two-dimensional Fourier transform electronic spectroscopy with a pulse-shaper," Opt. Express **16**, 17420–17428 (2008).
29. A. D. Bristow, D. Karaiskaj, X. Dai, T. Zhang, C. Carlsson, K. R. Hagen, R. Jimenez, and S. T. Cundiff, "A versatile ultrastable platform for optical multidimensional fourier-transform spectroscopy," Rev. Sci. Instrum. **80**, 073108 (2009).
30. W. Warren and A. Zewail, "Multiple phase-coherent laser pulses in optical spectroscopy. I. The technique and experimental applications," J. Chem. Phys. **78**, 2279 (1983).
31. J. Helbing and P. Hamm, "A compact implementation of Fourier transform 2D-IR spectroscopy without phase ambiguity," J. Opt. Soc. Am. B (submitted).
32. M. Bonmarin and J. Helbing, "Polarization control of ultrashort mid-IR laser pulses for transient vibrational circular dichroism measurements," Chirality **21**, E298–E306 (2009).
33. F. Dostal, "Resonant torsional oscillators - patent 3609485," United States Patent (1969).

1. Introduction

In recent years, 2D IR spectroscopy has developed rapidly into a powerful technique for studying structural dynamics of increasingly large and complex molecules [1–19]. For the application of 2D IR spectroscopy to low concentration analytes such as proteins, signal-to-noise and signal-to-background ratios place constraints on what systems can be studied. The challenge is to develop experimental setups that produce the strongest 2D IR signal and measure it with the minimum amount of signal loss. A number of experimental techniques have been developed for acquiring 2D IR spectra, each with their own balance of simplicity, flexibility and signal-to-noise levels [19].

In this paper, we focus on experimental arrangements where the 2D IR signal can be spatially isolated from the three incident beams through phase matching and then heterodyne detected using a separate local oscillator pulse (which, for brevity, we will denote loosely as a 'box-CARS' arrangement). The box-CARS geometry allows for the most flexible control of all pulse

#136705 - $15.00 USD Received 20 Oct 2010; revised 11 Nov 2010; accepted 16 Nov 2010; published 8 Dec 2010

parameters, and is, at the same time, potentially the most sensitive 2D IR setup. However, not only the desired heterodyned 2D IR signal is measured but also unwanted contributions which originate from interference between scattered light of any pairwise combination of the three incident beams, the local oscillator and the signal field. Scattering occurs when imperfections in the windows are present (scratches, fingerprints), when the sample is impure or when the sample is intrinsically scattering (polycrystalline materials [20], macroscopic aggregates [21]). The scattering signal appears on the diagonal of the 2D IR spectrum and adds significantly to the challenge of measuring small signals.

In most realizations of 2D IR spectroscopy, an optical chopper is used to block one of the incident beams every other laser shot. By taking the difference between the two measurements, all contributions that are present in both measurements (i.e. all combinations except those which include the chopped beam) will be removed, while the signal remains. However, chopping comes at a high price, as the signal is measured only every other laser shot. Furthermore, it does not remove scattering contributions involving the chopped pulse.

In NMR spectroscopy, carefully chosen phase-cycling sequences are used to select certain contributions and remove others [22]. In short, if the phase difference between two measurements is π, the sign of the two measurements is opposite and a subtraction will result in double the signal of a single measurement while an addition will result in total elimination. Comparable schemes have been implemented for the optical counterparts, see for example Wiersma and coworkers [23], Jonas [24], Warren [25], Marcus [26], Zanni [18, 27], Ogilvie [28] and Cundiff [29]. While phase shifts and pulse delays are completely independent in NMR sequences, this is not necessarily the case for optical spectroscopy (Fig. 1). With a pulse shaper or an acoustic optical modulator (AOM), phase and delay can in fact be modulated independently [30]. If some of the pulses are collinear, as in a pump/probe 2D IR setup [18], a single pulse shaper can modulate the phase of two interactions [18, 27, 28]. Modulation of an experiment with four independent beams, such as a box-CARS 2D IR arrangement, would imply adding more pulse shapers or AOMs to achieve the necessary phase control, as for example Marcus does in the visible [26], with the drawback that IR AOM's are not very efficient (30-50%).

In this paper, we will present a simple quasi-phase-cycling scheme achieved by sub-cycle delay modulation, which makes full use of all available laser shots in order to maximize the 2D IR signal-to-noise ratio. A sub-cycle delay modulation is introduced by either a wobbling brewster window or a photo-elastic modulator (PEM), both of which modulate the optical path length. Despite the fact that these devices generate a sub-cycle pulse delay rather than a pure phase shift (Fig. 1a), we will show that they affect the desired 2D IR signal only minimally over a bandwidth of many 100 cm^{-1}, while at the same time completely suppressing all scattering contributions in a way similar to pure phase-cycling. These devices are simple to construct and can easily be incorporated into any existing 2D IR setup, as they do not redirect the beam path. Furthermore, they have essentially 100% throughput and do not cause any light losses. We focus our discussion on 2D IR spectroscopy, but the concepts will work equally well in the visible or UV spectral range.

2. Theory

We describe all relevant laser fields in the time domain as

$$E(t) = \tilde{E}(t)e^{-i(\omega_0 t+\phi)}, \tag{1}$$

where $\tilde{E}(t)$ is the envelope, ω_0 the carrier frequency and ϕ the phase. The frequency domain representation of this pulse is:

$$E(\omega) = \tilde{E}(\omega)e^{-i(\omega t_0+\phi)}, \tag{2}$$

#136705 - $15.00 USD Received 20 Oct 2010; revised 11 Nov 2010; accepted 16 Nov 2010; published 8 Dec 2010

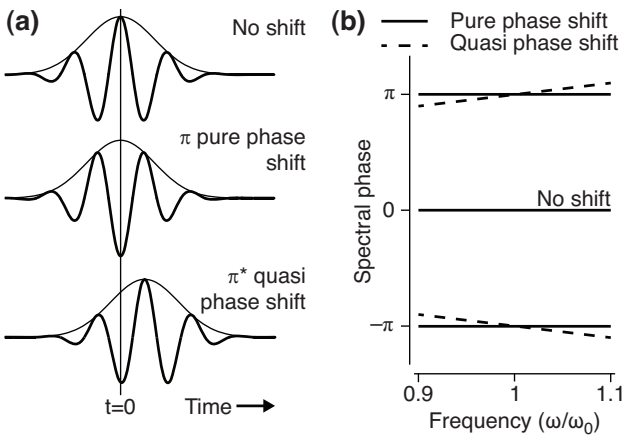

Fig. 1. A pure π phase shift versus a quasi-phase shift achieved by a sub-cycle delay. (a) In the time domain, a pure π phase shift will move the carrier only but keeps the pulse envelope constant in time. A quasi-phase shift, in contrast, will move both the envelope and the carrier. (b) In the frequency domain, the spectral phase of a pure phase modulation is independent of the frequency (solid line). A quasi-phase shift will have a spectral phase that varies linearly with frequency (dotted line).

where t_0 is the time delay of the pulse, and where we assume $\tilde{E}(\omega)$ to be real-valued (i.e. a bandwidth-limited pulse). For spectral interferometry, the interference between any pair of pulses *i* and *j* is given as

$$|E_i(\omega)+E_j(\omega)|^2=\tilde{E}_i^2(\omega)+\tilde{E}_j^2(\omega)+2\tilde{E}_i(\omega)\tilde{E}_j(\omega)\cos(\omega\Delta t+\Delta\phi) \tag{3}$$

where Δt the time delay difference between the two pulses and $\Delta\phi$ the phase difference. We are only interested in the cross term, which we define as

$$S_{ij}(\Delta t,\Delta\phi)\equiv\tilde{E}_i(\omega)\tilde{E}_j(\omega)\cos(\omega\Delta t+\Delta\phi) \tag{4}$$

In this expression, pulses E_i and E_j can be any pairwise combination of the incident pump pulses E_1, E_2, E_3, the local oscillator E_{LO}, and the signal field E_{2DIR}.

In a heterodyne detected 2D IR experiment (Fig. 2), three incident fields E_1, E_2, E_3 with different *k*-vectors k_1, k_2 and k_3 interact with the sample and generate the signal field E_{2DIR}, which is emitted in a certain phase matching direction ($k_{2DIR}=\pm k_1\mp k_2+k_3$). It is then heterodyned with the local oscillator by spectral interferometry, Eq. (4), to give $E_{2DIR}E_{LO}$. This term is measured as a function of t_1 by scanning pulses 1 and/or 2 in time and Fourier transforming it to obtain the ω_1 axis of the 2D spectrum, while the Fourier transformation with respect to time t_3, revealing the ω_3 axis, is measured directly using a grating spectrometer and an array detector.

In addition to the desired $E_{2DIR}E_{LO}$ term, many other interference terms are present on the detector. These originate from scattered light so phase-matching can no longer be used to eliminate them. For example, pulse 1 might scatter into the direction of the local oscillator and interfere on the detector, causing a signal E_1E_{LO}. As time t_1 is scanned during the experiment, this signal will oscillate according to Eq. (4) (Δt equals $t_1+t_2+t_3$ in this case), and will give rise to a signal along the diagonal of the 2D IR spectrum after the t_1-Fourier transformation. The goal of this work is to suppress these types of signals.

#136705 - $15.00 USD Received 20 Oct 2010; revised 11 Nov 2010; accepted 16 Nov 2010; published 8 Dec 2010

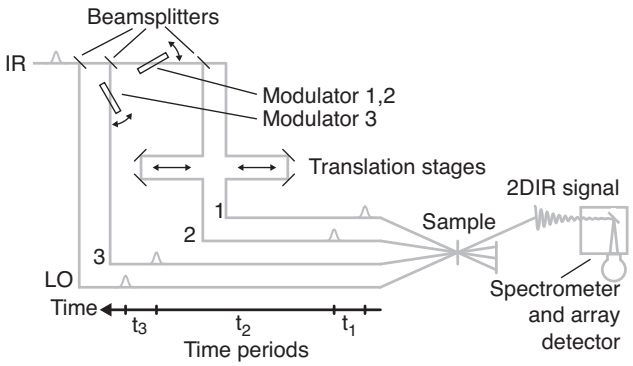

Fig. 2. A schematic drawing of the box-CARS 2D IR setup. An IR pulse is split into four pulses E_1, E_2, E_3 and E_{LO}. Pulses 1 and 2 are transmitted together through one modulator before they are split, while pulse 3 is modulated independently. The three incident pulses generate the signal field E_{2DIR}, which is heterodyned with the local oscillator by spectral interferometry. The timing notation is defined at the bottom of the figure.

Finally, we note that depending on the phase matching geometry, pump-probe signals can be present as well. They are 3rd-order signals that take two field interactions from either of the pump-pulses 1, 2, or 3, and use the local oscillator for both the 3rd field interaction as well as heterodyning. The pump-probe signals are inherently not phase sensitive, thus are *not* oscillatory. They will appear at essentially zero-frequency after the t_1-Fourier transformation, and hence are not so much of a concern here because they will be suppressed anyway. Nevertheless, the phase-cycling schemes described below will also suppress these pump-probe contributions.

2.1. Simple phase-cycling scheme

In order to illustrate the basic concept of phase-cycling, and also the difference between a pure phase shift and quasi-phase shift achieved through sub-cycle delay modulation, we start out with a simple phase-cycling scheme that modulates only pulse 3. That is, pulse 3 will have phase $\phi_3 = 0$ for one laser shot, and phase $\phi_3 = \pi$ for the next. The phase of the signal field E_{2DIR} depends on the phases of all three incident pulses:

$$\phi_{2DIR} = \pm\phi_1 \mp \phi_2 + \phi_3, \tag{5}$$

hence, it will have the same phase as ϕ_3 and thus will be modulated as well in this phase-cycling scheme. Subtracting the two measurements results in

$$\begin{aligned} \tilde{S}_{2DIR,LO}(\Delta t) &= S_{2DIR,LO}(\Delta t, \Delta\phi = 0) - S_{2DIR,LO}(\Delta t, \Delta\phi = \pi) \\ &= 2\tilde{E}_{2DIR}(\omega)\tilde{E}_{LO}(\omega)\cos(\omega\Delta t) \end{aligned} \tag{6}$$

Since the sign of the two measurements is opposite due to the π-phase shift in the second measurement, subtraction will double the signal.

The optical devices we discuss below cause a sub-cycle delay modulation δt rather than a pure phase modulation (Fig. 1a). Equation (4) then becomes

$$S_{ij}(\Delta t + dt) = \tilde{E}_i(\omega)\tilde{E}_j(\omega)\cos(\omega(\Delta t + \delta t)). \tag{7}$$

#136705 - $15.00 USD Received 20 Oct 2010; revised 11 Nov 2010; accepted 16 Nov 2010; published 8 Dec 2010

where we assumed that the pure phase difference is $\Delta\phi = 0$. In effect, the sub-cycle delay modulation δt will take over the role of a phase shift $\Delta\phi$. That is, we will use a time delay δt that equals half an optical period of the carrier frequency, $\delta t = \pi/\omega_0$. This will result in a spectral phase that equals π at the center of the pulse bandwidth ($\omega = \omega_0$) but will deviate linearly from π for $\omega \neq \omega_0$ (Fig. 1b). Equation (6) is then modified into

$$\begin{aligned} \tilde{S}_{2DIR,LO}(\Delta t) &= S_{2DIR,LO}(\Delta t) - S_{2DIR,LO}(\Delta t + \pi/\omega_0) \\ &= 2\tilde{E}_{2DIR}(\omega)\tilde{E}_{LO}(\omega)\sin\left(\omega\Delta t + \frac{\pi\omega}{2\omega_0}\right)\sin\left(\frac{\omega\pi}{2\omega_0}\right). \end{aligned} \tag{8}$$

The oscillatory term is slightly different (in fact we have $\sin(\omega\Delta t + \pi\omega/2\omega_0) \approx \cos(\omega\Delta t)$ for $\omega \approx \omega_0$), but more important is the additional $\sin(\omega\pi/2\omega_0)$-term, which can be interpreted as a spectral response. For the center frequency of the pulse ($\omega = \omega_0$), the spectral response is 1 and the pure and quasi-phase shift have the same amplitude. For off-center frequencies $\omega \neq \omega_0$, the spectral response is < 1. However, the signal reduction is very small, less than 1.2% for a frequency window of $\pm 10\%$ around the center frequency. For convenience, we will call a sub-cycle delay of $\delta t = \pi/\omega_0$ a quasi-phase shift $\Delta\phi^* = \pi^*$ in the following, where the asterisk denotes that this is strictly correct only for $\omega = \omega_0$.

We reiterate that both pure and quasi-phase modulation will double the 2D IR signal compared to a configuration with a chopper, simply because the signal is measured every single laser shot while the chopper wastes half of them. At the same time, the subtraction will suppress, for example, the scattering term E_1E_{LO}, since neither pulses 1 nor the local oscillator are phase modulated, hence do *not* change sign in the two measurements. The same holds for E_2E_{LO}. In contrast, the scattering term E_3E_{LO} is not suppressed; in fact it is amplified just like the 2D IR signal. Nevertheless, this term is not modulated as time t_1 is scanned, hence it appears at zero frequency after the t_1-Fourier transform and is suppressed this way. It is therefore crucial to put a single phase-modulator into beam 3, and not beam 1 or 2.

However, there are additional scattering terms that will not be suppressed by this simple phase-cycling scheme. Consider for example the term E_1E_3, which originates from interference of light scattered from pulse 1 with light scattered from pulse 3. Pulse 3 is phase-modulated in this scheme, hence the sign of E_1E_3 is inverted just like that of the desired 2D IR signal, and the intensity of this scattering term is actually doubled. A chopper would not suppress this type of signal either. One might assume that E_1E_3 is small because it is the interference between two scattered and thus weak fields. However, pulses 1 and 3 are intense, whereas the local oscillator is typically much weaker, hence we observe in our lab that scattering terms like E_1E_3 are actually not so much smaller than scattering terms like E_1E_{LO}, and severely disturb 2D IR spectra as well. In the next section, we will introduce a quasi-phase-cycling scheme that eliminates all scattering terms.

2.2. Double phase-cycling

To remove all scattering terms, we introduce a second modulator that phase-shifts pulses 1 and 2 together, while pulse 3 is modulated independently. The cycle is now periodic over 4 measurements. The upper part of Tab. 1 shows the states of the two modulators during these four measurements and the signs with which they contribute to the final signal (see also Fig. 3a). We will compare two sequences which differ by ϕ_3 in the fourth measurement that is either $+\pi^*$ or $-\pi^*$. If these were pure phase shifts, then $+\pi$ and $-\pi$ would of course be identical, but the same is not true for quasi-phase shift. We will see that a $-\pi^*$ quasi-phase shift leads to an exact suppression of all scattering terms for all frequencies. A $+\pi^*$ quasi-phase, in contrast, suppresses them only at $\omega = \omega_0$, with the scattering amplitude rising linearly around the center

#136705 - $15.00 USD Received 20 Oct 2010; revised 11 Nov 2010; accepted 16 Nov 2010; published 8 Dec 2010

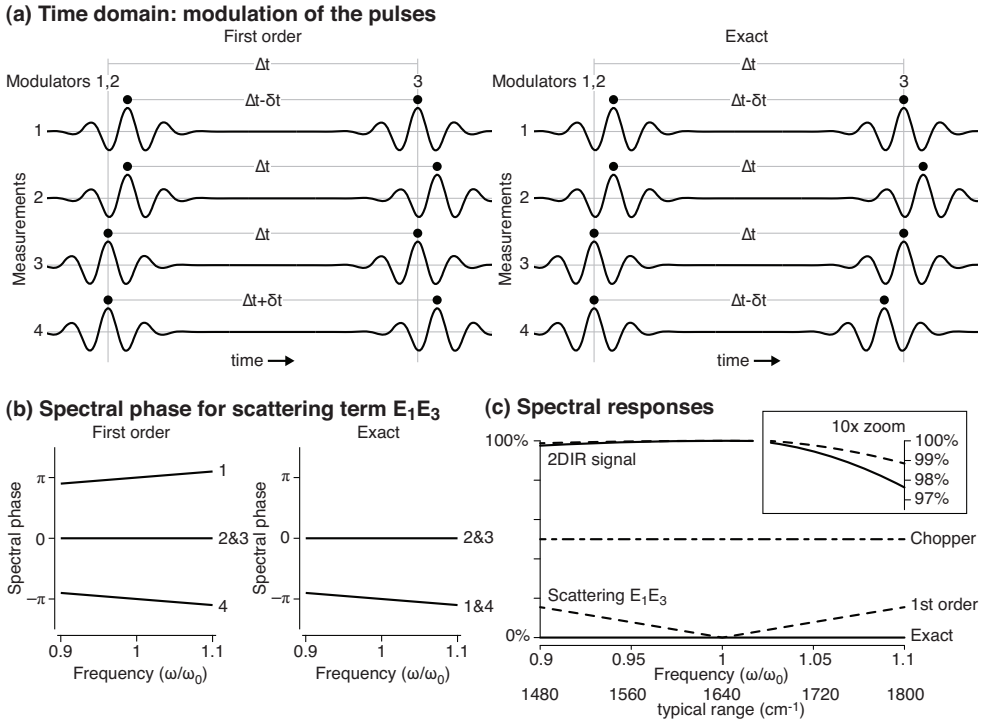

Fig. 3. Comparison of exact and first-order sequences. (a) The positions of the pulses in time for the four measurements. (b) The spectral phases of the four measurements exemplified by the scattering term E_1E_3. (c) Spectral responses. A chopper measures the 2D IR signal only for every other laser shots, hence the overall signal is half. With quasi-phase-cycling, every laser shot is used, so the signal is larger, but a tiny frequency dependence of the response is present (see Eqs. (11) and (12)). The exact sequence will completely eliminate scattering (see Eq. (9)), while scattering will rise linearly off the center frequency for the the first-order sequence (see Eq. (10)).

frequency. We therefore will call the former sequence the 'exact sequence' while we refer to the latter as a 'first-order sequence' (higher order suppression can be achieved in this case as well, see Ref. [31]).

We demonstrate the scattering suppression for the specific case of E_1E_3, though the result is general. Measured with the exact sequence, we obtain:

$$\begin{aligned}\tilde{S}_{13}(\Delta t) &= +S_{13}(\Delta t, \Delta\phi^* = +\pi^*) - S_{13}(\Delta t, \Delta\phi^* = 0) \\ &\quad +S_{13}(\Delta t, \Delta\phi^* = 0) - S_{13}(\Delta t, \Delta\phi^* = +\pi^*) = 0 \end{aligned} \tag{9}$$

where $\Delta\phi^*$ is the overall spectral phase of that term (Tab. 1). The first and fourth measurement make a pair with the same time delay $\Delta t - \delta t$, so do the second and third measurement with time delay Δt (Fig. 3a, right panel). The frequency domain equivalent of this statement is depicted in Fig. 3(b), right panel: pairwise two measurements with identical spectral phases are subtracted, hence the elimination of the scattering term is exact (Fig. 3c).

In contrast, the first-order sequence eliminates scattering only incompletely. That is, the second and third measurement again form a pair that exactly cancels, but the first and fourth measurement have different time delays $\Delta t \pm \delta t$ (Fig. 3a, left panel), or opposite spectral phases

#136705 - $15.00 USD Received 20 Oct 2010; revised 11 Nov 2010; accepted 16 Nov 2010; published 8 Dec 2010

Table 1. The states of the two modulators for the four measurements of the phase cycle (row 2-3) and the sign (row 4) with which they contribute to the final signal. For the fourth measurement, two different phase-shifts are introduced for ϕ_3, leading to the first-order ($\phi_3 = \pi^*$) and the exact ($\phi_3 = -\pi^*$) sequence, respectively. The first column lists all possible combinations of fields that may interfere on the detector, the second column the overall phase of this term which is then spelled out in column (3-7) for each of the four measurements of the cycle. The two right-most columns list the final signal for the first-order and the exact sequence, respectively. The asterisk means that the result is not exact when quasi-phase shifts are used, i.e. 0^* refers to Eq. (10) and 1^* to Eq. (11) or Eq. (12), respectively.

		Measurement						
		1	2	3	4			
Phase $\phi^*_{1,2}$		π^*	π^*	0	0			
Phase ϕ^*_3		0	π^*	0	$+\pi^*$	$-\pi^*$		
Sign		$+$	$-$	$+$	$-$			
Fields	Overall phase $\Delta\phi^*$						1^{st}-ord	Ex.
E_1E_2	$\phi_1-\phi_2$	0	0	0	0	0	0	0
E_1E_3, E_2E_3	$\phi_1-\phi_3, \phi_2-\phi_3$	π^*	0	0	$-\pi^*$	$+\pi^*$	0^*	0
E_1E_{2DIR}, E_2E_{2DIR}	$\phi_1-\phi_{2DIR}, \phi_2-\phi_{2DIR}$	π^*	0	0	$-\pi^*$	$+\pi^*$	0^*	0
E_1E_{LO}, E_2E_{LO}	$\phi_1-\phi_{LO}, \phi_2-\phi_{LO}$	π^*	π^*	0	0	0	0	0
E_3E_{LO}	$\phi_3-\phi_{LO}$	0	π^*	0	$+\pi^*$	$-\pi^*$	1^*	1^*
E_3E_{2DIR}	$\phi_3-\phi_{2DIR}$	0	0	0	0	0	0	0
$E_{2DIR}E_{LO}$	$\phi_{2DIR}-\phi_{LO}$	0	π^*	0	π^*	$-\pi^*$	1^*	1^*

(Fig. 3b, left panel), respectively. Hence, their subtraction does not eliminate the scattering contribution completely. The remaining scatter of E_1E_3 is:

$$\begin{aligned}\tilde{S}_{13}(\Delta t) &= +S_{13}(\Delta t,\Delta\phi^*=+\pi^*)-S_{13}(\Delta t,\Delta\phi^*=0)\\ &\quad +S_{13}(\Delta t,\Delta\phi^*=0)-S_{13}(\Delta t,\Delta\phi^*=-\pi^*)\\ &= -2\tilde{E}_1(\omega)\tilde{E}_3(\omega)\sin(\omega\Delta t)\sin\left(\frac{\omega\pi}{\omega_0}\right) \qquad (10)\end{aligned}$$

For the center frequency $\omega=\omega_0$, the second sine-term is zero and the scatter is eliminated. However, around the center frequency the sine term rises linearly and scatter elimination will be incomplete (Fig. 3c). For a frequency that is $\pm 10\%$ off-center, roughly 15% of the scatter remains.

Table 1 summarizes what we have just demonstrated for E_1E_3. For the exact sequence, all possible scattering terms are eliminated exactly for all frequencies despite the fact that we achieve only a quasi-phase shift. The only exception is E_3E_{LO}, however, this term will be eliminated after the t_1-Fourier transformation, as discussed earlier.

For the 2D IR signal, the exact sequence will reveal a response

$$\begin{aligned}\tilde{S}_{2DIR,LO}(\Delta t) &= +S_{2DIR,LO}(\Delta t,\Delta\phi^*=0)-S_{2DIR,LO}(\Delta t,\Delta\phi^*=+\pi^*)\\ &\quad +S_{2DIR,LO}(\Delta t,\Delta\phi^*=0)-S_{2DIR,LO}(\Delta t,\Delta\phi^*=-\pi^*)\\ &= 4\tilde{E}_{2DIR}(\omega)\tilde{E}_{LO}(\omega)\cos(\omega\Delta t)\sin^2\left(\frac{\pi\omega}{2\omega_0}\right) \qquad (11)\end{aligned}$$

that varies slightly more with frequency than the first-order sequence:

$$\tilde{S}_{2DIR,LO}(\Delta t) = +S_{2DIR,LO}(\Delta t,\Delta\phi^*=0)-S_{2DIR,LO}(\Delta t,\Delta\phi^*=+\pi^*)$$

#136705 - $15.00 USD Received 20 Oct 2010; revised 11 Nov 2010; accepted 16 Nov 2010; published 8 Dec 2010

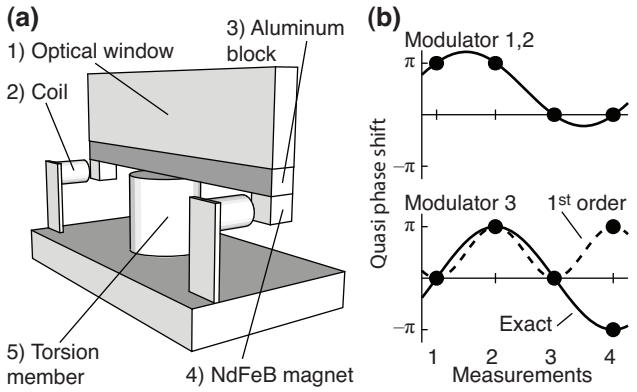

Fig. 4. (a) An optical window mounted on an electromagnetically driven torsional oscillator for use as a pulse delay modulator. (b) The upper panel shows the oscillation of modulator 1,2, the lower panel shows the modulation of modulator 3. For the exact sequence (solid line) the modulator has a $\pm\pi^*$ amplitude at a quarter of the laser repetition rate. For the first-order sequence (dashed line), the amplitude is π^* with half the laser repetition rate.

$$\begin{aligned} & +S_{2DIR,LO}(\Delta t, \Delta\phi^* = 0) - S_{2DIR,LO}(\Delta t, \Delta\phi^* = +\pi^*) \\ = \quad & 4\tilde{E}_{2DIR}(\omega)\tilde{E}_{LO}(\omega)\sin\left(\omega\Delta t + \frac{\pi\omega}{2\omega_0}\right)\sin\left(\frac{\pi\omega}{2\omega_0}\right) \end{aligned} \tag{12}$$

Again, we have $\sin(\omega\Delta t + \pi\omega/2\omega_0) \approx \cos(\omega\Delta t)$ for $\omega \approx \omega_0$. For the first-order sequence, the spectral response, $\sin(\pi\omega/2\omega_0)$, varies by ≈1.2% within a frequency window of ±10% around the center frequency, while that of the exact sequence, $\sin^2(\pi\omega/2\omega_0)$, varies by ≈2.4% (Fig. 3c). In both cases, this is a much smaller effect than that imposed by the spectral intensity of, for example, a 50 fs pulse, whose FWHM would be roughly ±10% (i.e. 300 cm^{-1}) at $\omega_0 = 1600\ \text{cm}^{-1}$.

3. Experimental

3.1. Wobbling brewster window

Mounting a window on a resonant torsional oscillator to tilt it periodically is a simple and robust method to rapidly modulate the delay of a laser pulse train with controlled frequency, phase and amplitude. The major design parameters are $\Delta\theta$, the torsion angle required to generate an appropriate delay change δt, the moment of inertia I of the entire rotor and κ, the spring constant of the oscillator (giving the resonance frequency $f = \sqrt{\kappa/4\pi^2 I}$). The delay time modulation $\delta t/\Delta\theta$ increases with increasing overall window angle θ, so it is convenient to rotate the window about the Brewster angle. For example, a 3 mm thick ZnSe Brewster mounted window (≈ 67.6° at λ=6 μm) will, when rotated by $\Delta\theta = \pm 0.07°$ make a delay δt equivalent to plus/minus half an optical cycle for an infrared pulse of 6 μm center wavelength.

Figure 4(a) shows schematically a typical device. An optical window (1) is glued to an aluminum block (3). Also glued onto each end of the block (4) are 3.2 mm square NdFeB magnets. The block is then attached either mechanically or with glue to a torsion member (5), itself clamped to a mounting block firmly secured to the optical bench. Driver coils (2) (10 μH, $I_{max} \approx 0.14$ A DC) are positioned to within 1 mm of the oscillator magnets, with one coil used to drive the oscillator and the other as a pickup for diagnostic purposes. The torsion members

#136705 - $15.00 USD Received 20 Oct 2010; revised 11 Nov 2010; accepted 16 Nov 2010; published 8 Dec 2010

tested here are single ended pivot (flexure) bearings (Riverhawk) and thin stainless steel tubes. A flexure bearing is an arrangement of stainless steel spring leafs connecting two independently rotating cylinders, allowing limited low friction torsional movement of one of these cylinders.

In the device we constructed, the ZnSe window had dimensions $3 \times 1 \times 0.3$ cm^3. The flexure bearing had a factory specified spring constant and moment of inertia of 21 N cm/degree and 4.4 g cm^2, respectively. The total moment of inertia of the bearing, window, magnets and aluminum block together was 8.2 g cm^2, giving a resonance frequency of 550 Hz with a width of a few Hz. For the 1 kHz repetition rate lasers used in our experiments, the modulator resonance was adjusted to ≈500 or 250 Hz by adding mass to the aluminum block. When using a steel tube as torsion member, in contrast, the spring constant of a tube with length L and shear modulus G is $\kappa = G\pi(D^4 - d^4)/32L$ (where D and d are the outer and inner diameters, respectively). Therefore the resonance frequency can be adjusted simply by changing the length of the tube protruding from the mounting block. For the devices tested, the coils and magnets used are capable of driving both torsion members at amplitudes of several degrees with drive levels of less than 10 V. This corresponds to tens of optical cycles scanned at 6 μm.

The devices are driven by a square wave with either 250 or 500 Hz, divided down from the regenerative amplifier 1 kHz Pockels cell trigger (since oscillation of the wobbler is a resonance effect, driving it with a square wave results in a sine-modulation). A tunable delay is used to adjust the wobbler's phase relative to the Ti:S laser pulse train, and a tunable gain amplifier to adjust the amplitude of the modulation. Adjustments of these parameters are made during operation of the 2D IR experiment to optimize for signal and at the same time minimize scatter.

3.2. Photo elastic modulator

For higher laser repetition rates, a Photo Elastic Modulators (PEM) can be used. A PEM compresses and stretches a crystal at its acoustic resonance frequency. The two extremes have opposite birefringence and act as waveplates in perpendicular directions. PEMs are commonly used as a way to change the polarization of a beam but can also be used to introduce a quasi-phase shift by orienting the modulation induced optical axis parallel or perpendicular to the beam polarization. The crystal is driven at its sharply defined resonance frequency and is factory-set for an individual device. This makes it necessary to synchronize the laser to the PEM [32]. For the simple two-cycle scheme (Sect. 2.1), the laser frequency is derived from the PEM frequency as $f_{Laser} = 2f_{PEM}/(2n+1)$, using a phase locked loop (PLL, to double f_{PEM}) and a subsequent divider by an odd number. The integer number n is chosen such that the repetition rate f_{Laser} closely matches that for which the Ti:S amplifier is optimized. In this way, one laser shot will see one extreme of the crystal oscillation, and the next laser shot the other extreme (after a proper phase adjustment of the oscillation).

A ZnSe based PEM (Hinds Instruments) with a resonance frequency of 50 kHz is used here. The modulation depth of this PEM is sufficient to achieve a π quasi phase shift for wavelengths less than 6.5 μm. Anti reflective coating of the ZnSe crystal gives 80-90% transmittance between 3 and 6 μm. In principle, a 50 kHz resonance allows for laser repetition rates of up to 100 kHz (i.e. $n = 0$), or even 200 kHz if the four phase-cycle sequence is used. However, in the latter case, two PEM's have to be synchronized to each other.

3.3. Experimental verification

The quality of scattering elimination was tested using two wobbling brewster windows. Pulses 1 and 3 (with a pulse separation of $\Delta t \approx 1.5$ ps) were scattered from a 30 μm pinhole and their

#136705 - $15.00 USD Received 20 Oct 2010; revised 11 Nov 2010; accepted 16 Nov 2010; published 8 Dec 2010

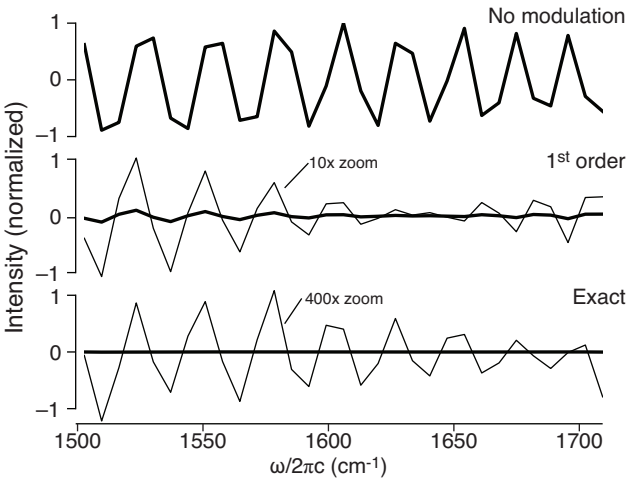

Fig. 5. Experimental scattering elimination using the first-order and the exact sequences. (Top)) Original scattering signal, (middle) suppression using the first-order sequence; the 10x zoom (thin line) illustrates that the elimination is complete only for the center frequency (around 1640 cm^{-1}). (Bottom) Exact sequence, which reduces the scattering by a factor 400.

interference was measured on an array detector. Both the first-order and the exact sequences have been implemented. In the first case, modulator 3 produced a π^* phase shift at 500 Hz (i.e. half the laser repetition rate, see Fig. 4(b), lower panel, dotted line) and modulator 1,2 a π^* phase shift at 250 Hz (Fig. 4b, upper panel). In the second case, modulator 3 produced a $\pm\pi^*$ phase shift at 250 Hz (Fig. 4b, lower panel, solid line). Note that both the wobbling brewster window and the PEM can only produce a sine-shaped delay modulation, since these are resonant oscillators. However, by introducing a proper amplification and delay for modulator 1,2, the required quasi-square modulation with $\phi_{1,2} = (\pi^*, \pi^*, 0, 0)$ can be realized (Fig. 4b, upper panel).

Figure 5 summarizes the results of these experiments. The full scattering amplitude E_1E_3 Eq. (4) is shown in the upper panel, and its suppression by the first-order sequence in the middle panel. The suppression is complete for the center frequency (1640 cm^{-1} in this case), but the scattering amplitude increases linearly around it according to Eq. (10). In contrast, the exact sequence suppresses the scattering by more than a factor 400 (see Eq. (9) and Fig. 5, lower panel). The remaining signal can be attributed to the slight non-linearities in $\delta t/\Delta\theta$, the precision to which the amplitudes of the modulators can be matched, and the small lateral offset introduced by the wobbling Brewster windows.

4. Discussion and conclusions

As has been stressed before by many authors [18, 24, 30], delay modulation and phase modulation are the same only for monochromatic light. For short pulses with non-negligible $\Delta\omega/\omega$, the spectral phase becomes important and makes the design of a pulse sequence more complicated. Nevertheless, as we demonstrate in this paper, by properly placing and operating sub-cycle delay modulators, one can double the 2D IR signal (compared to a configuration with a chopper). The signal deviates very little from what would be obtained by pure phase-cycling, with a spectral response variation that is much smaller than that originating form the limited bandwidth of

#136705 - $15.00 USD Received 20 Oct 2010; revised 11 Nov 2010; accepted 16 Nov 2010; published 8 Dec 2010

the pump pulses. Furthermore, population time t_2 is modulated as well, effectively reducing the t_2-time resolution by 10 fs for 6 μm light. At the same time, all possible scattering contribution are suppressed exactly for all frequencies, despite the fact that only a quasi-phase-cycling is achieved. Both modulation devices discussed here (wobbling brewster window and PEM) are simple and can be implemented in essentially any existing 2D IR setup, as they do not require any change of the beam geometry. Furthermore, in particular the wobbling brewster window has practically no losses since the window is introduced in the Brewster angle.

Modulating the pulses on a shot-to-shot basis gives the best correlation between laser shots and hence the lowest possible noise. The home built phase modulator devices were designed to operate at the 250 Hz frequencies dictated by the 1 kHz amplifier. As higher laser repetition rates are becoming more common, we also investigated the feasibility of achieving higher modulator resonance frequencies. A $1 \times 1.5 \times 0.1$ cm^3 BK7 window mounted on an $L = 0.35$ cm tube was found to have a resonance frequency of 2.5 kHz and $\Delta\theta$ = 0.1 $^\circ$ for a 10 V drive level, indicating that based on the principles described here, suitable IR modulators may be constructed for laser systems running at up to 10 kHz. We note that a more complicated tapered rod design for mirror scanning is described in the literature that achieves large angular excursions at frequencies up to 10 kHz [33]. For repetition rates that are beyond the feasibility of a wobbling Brewster window, a PEM can be used.

We have restricted our discussion to infrared modulation. We note that for visible experiments, although modulator options are more varied (e.g AOMs, EOMs, liquid crystal modulators etc.) than for the infrared, the modulators proposed here offer a convenient and low cost alternative as well.

A detailed scheme of the wobbling Brewster window is available from the authors and will be developed into a kit for interested laboratories.

Acknowledgments

We would like to thank Jan Helbing for helpful discussions and Martin Haller for friendly technical support. This work was financially supported by an ERC advanced investigator grant (DYNALLO).

#136705 - $15.00 USD Received 20 Oct 2010; revised 11 Nov 2010; accepted 16 Nov 2010; published 8 Dec 2010